J Mater Sci (2015) 50:112–121
DOI 10.1007/s10853-014-8571-y

Role of a gradient interface layer in interfacial enhancement of carbon fiber/epoxy hierarchical composites

Lei Chen · Hao Jin · Zhiwei Xu · Jialu Li · Qiwei Guo · Mingjing Shan · Caiyun Yang · Zhen Wang · Wei Mai · Bowen Cheng

Received: 28 April 2014 / Accepted: 26 August 2014 / Published online: 23 September 2014

Abstract To improve the interfacial properties of carbon fibers/epoxy composites, we introduced a gradient interphase reinforced by graphene sheets between carbon fibers and matrix with a liquid phase deposition strategy. Interlaminar shear strength and flexural strength of the composites are both improved. The interfacial reinforcing mechanisms are explored by analyzing the structure of interfacial phase with linear scanning system of scanning electron microscope and atomic force microscope. Results indicate that carbon element shows a graded dispersion in the interface region and a gradient interface layer with the modulus decreasing from fibers and matrix is found to be built. To verify the effect of gradient interphase on the interfacial properties of composites, the mixture of carbon fiber/graphene/epoxy is sonicated before curing to disperse graphene sheets in matrix homogeneously. As a result, gradient interphase structures are disappeared and interfacial performance of composites is found to be weakened. The role of gradient interface layers in enhancing interfacial performances is further proved from a different angle.

Introduction

It is well known that the performance of the carbon fiber (CF)-reinforced composites is, to a large extent, controlled by the fiber-matrix interface. Good interfacial properties are essential to ensure efficient load transfer from fibers to matrix, which helps to reduce stress concentrations and improve overall mechanical properties [1, 2]. Attempts to improve the interlaminar fracture toughness and delamination fatigue properties of composites have so far shown various results. Many nano-fillers (carbon nanotubes, nanoclays, etc.) have been considered to be applied as the modifiers of the traditional composites in order to enhance the mechanical, thermal, electric, and gas/liquid barrier properties or to add multi-functionality [3–16]. The created chemical bonding and mechanical interlocking, increased fiber surface area, or local stiffening at the interface should be the main reasons for improving stress transfer and then interfacial properties [13, 17–22].

With low density and large specific surface area, graphene sheets (EG) have been widely used for the reinforcement of nanocomposites [23–27]. They were highly effective in suppressing crack propagation in polymer matrix, and resulted in improvement of strength and toughness of the polymer composites [24, 26, 28]. These properties make it an ideal candidate for using as the reinforcement in high-performance composites, especially in the fields of multi-scale composites [7]. In zhang et al work [1], graphene oxide sheets were directly introduced onto the CF surface and interfacial properties of composites were investigated by microbond test and three-point short beam shear test. Tests indicated a 36.3 % improvement of interfacial shear strength and a 12.7 % improvement of interlaminar shear strength (ILSS) compared with that of commercial-sizing-modified CF composites. In addition, the tensile strength and tensile modulus were also improved by introducing graphene oxide, which could be interpreted by the formation of chemical bridging between CF, graphene oxide sheets, and matrix [4]. Yavari et al [2] also found that over three orders of magnitude enhancement in flexural bending fatigue life of glass fiber-

L. Chen · H. Jin · Z. Xu (✉) · J. Li · Q. Guo · M. Shan · C. Yang · Z. Wang · W. Mai · B. Cheng
Key Laboratory of Advanced Braided Composites, Ministry of Education, School of Textiles, Tianjin Polytechnic University, Tianjin 300160, People's Republic of China
e-mail: xuzhiwei@tjpu.edu.cn

reinforced composites was achieved by graphene platelets. However, it is hard to determine that the increase in fatigue life should be attributed to improved interfacial properties or increased toughness of matrix.

In present work, we explore an approach to introduce a graphene-based gradient interface layer between CFs and epoxy to enhance the interface strength, which is different from the reported mechanisms of improving interfacial properties. Expanded EG were delivered to the surface of CF by a liquid phase deposition method [19]. Composites were prepared by resin transfer molding (RTM) technology. The ILSS of composites was investigated by short beam shear tests. Flexural properties of multi-scale composites were also detected to assure the modification of mechanical properties. Due to the micro-scale of components at interface, in combination with physical tests related to mechanical properties, force modulation atomic force microscope (AFM) tests and linear scanning of scanning electron microscope (SEM) were carried out, targeting to analyze the variation of interfacial structures. For further investigation of reinforcing mechanisms, after injection of resin, the mold was sonicated so that graphene fillers can be penetrated into matrix extensively. The mixtures were then cured and the sonicated composites were prepared. The interfacial properties and the fiber/matrix interface structures of sonicated composites were also characterized and compared with the pristine and hierarchical composites to identify the exact reinforcing mechanisms.

Experimental section

Preparation of EG

The EG were prepared by expanding the graphite oxide in high temperature. The graphite oxide was firstly prepared according to the method as described by Marcano et al. in [29]. A 9:1 mixture of concentrated H_2SO_4/H_3PO_4 (720:80 mL) was added to a mixture of graphite flakes (6.0 g, carbon content >99.99 %) and $KMnO_4$ (18.0 g), producing a slight exotherm to 35–40 °C. The mixture was then heated to 50 °C and stirred for 12 h. The mixture was cooled to room temperature and poured onto ice (800 mL) with 30 % H_2O_2 (6 mL). After then, the mixture was filtered over a polytetrafluoroethylene membrane with a 0.22 μm pore size. The remaining solid was then washed in succession with 2000 mL deionized water. For each wash, the mixture was centrifuged at a speed of 8000 rpm. The solid obtained in the centrifuge tube was then freeze-dried at room temperature to get graphite oxide powder. The quartz tube with graphite oxide powder was quickly inserted into a furnace preheated to 1000 °C and held in the furnace for 1 min to get EG [30].

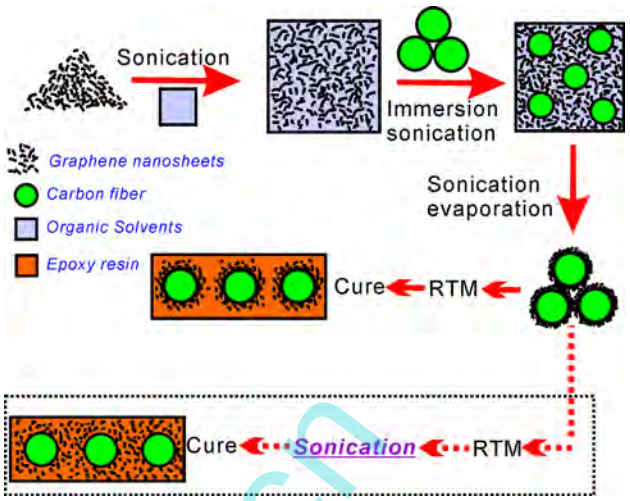

Fig. 1 Schema illustration for the preparation of CF absorbed with EG

Preparation of EG-coated CF and composites

Figure 1 shows the procedure for preparation of CNS-coated CF and composites. To exclude possible effects of commercial size from the ILSS improvement in the system, we refluxed the commercial CF (T700S from Jiangsu Tianniao Co., LTD) with acetone and petroleum benzin for 24 h beforehand. Firstly, different weights of EG were dispersed in acetone under sonication with a concentration of 0.5 mg/ml and the washed CF was then immersed into the solution. The mixture was sonicated for 2 h to promote the absorption of EG onto CF. Secondly, the bath was heated to 100 °C under sonication to evaporate organic solvents and the CF absorbed with various contents of EG (0.1, 0.3, 0.5, 1.0, 1.5, 2.0 wt% relative to composites) was prepared.

The composites were produced via the RTM process. As fiber-reinforcement, the as-prepared unidirectional CF was used. The fiber volume fraction was chosen as high as 60 % so that the EG cannot be flushed out during the injection of resin. An epoxy resin system (Guangzhou Yigao Co., LTD.) with the anhydride hardener (Zhejiang Qingan Co., LTD.) was used as matrix polymer in this study. The resin was preheated at 60 °C and 2 h of injection was carried out to minimize void defects. The pressure of mold was controlled precisely and sample sizes were measured to make sure that fiber volume fractions of samples were equivalent to each other. After infusion, the mold was cured at 90 °C for 3 h, 120 °C for 3 h, and then 150 °C for 5 h. Samples with obvious resin-rich field will

be discarded. Furthermore, in order to improve the distribution of EG in composites, the mold with fibers and resins was sonicated before curing (as shown in dashed box in Fig. 1). The sonicated composites were then reached by heating the sonicated mold.

Characterizations and tests

Tapping mode of AFM (CSPM 5500 from Guangzhou Benyuan LTD.) was used to observe the morphology and the thickness of EG. In addition, the chemical structure of EG was determined by X-ray photoelectron survey (XPS, Thermo ESCALAB 250) spectra.

The short beam shear tests were carried out according to JC/T773-2010 to determine the effect of EG and their content on ILSS. All tests were carried out at room temperatures and the reported values were calculated as averages of five specimens for each composite. Flexural properties of the composites were measured according to GB/T1449-2005. Both of these tests were performed in an Instron mechanical testing machine (Instron5567, USA) using a cross-head speed of 1 mm/min. Furthermore, the morphologies of fracture surfaces of pristine and modified composites were observed with SEM.

Linear scanning system of SEM (JEOL JSM-5900LV) was applied to detect the carbon element distribution in the interface layers. The SEM samples were coated with a thin layer of gold prior to examinations. In addition, force modulation mode of AFM was adopted to study the stiffness of various phases to evaluate the exact structures of interface layers. A silicon nitride probe with the spring constant of 5 $N \cdot m^{-1}$ and the resonant frequency of 70–150 kHz was selected. For observing the stiffness of interface accurately, the cross-sections of composite specimens were polished using sand papers and a Cr_2O_3 suspension with an average grain size of 50 nm, cleaned with water in ultrasonic washer and dried.

Results and discussion

Microstructural characterizations of EG

We first examine the morphology of EG by AFM. The thickness of EG we prepared is within a range of 1.6–2.1 nm, as indicated in Fig. 2b. The layers of EG should be mostly less than five due to the fact that the monolayer is somewhat larger than theoretical thickness (0.34 nm) of parent graphene because of the folding of monolayer EG. The sheets are a little more 'bumpy' than predicted, which is possibly due to the existence of wrinkle. Note the wrinkled (rough) surface texture of EG which could play an important role in enhancing mechanical interlocking and load transfer with matrix. XPS spectra of graphite oxide and EG are presented in Fig. 2c. Spectrum of graphite oxide indicates the presence of abundant oxygen groups. After reduction, absorption of EG at infrared range is not observable, likely due to the exhaustive reduction of graphite oxide.

Surface topography of modified CF

Surface morphologies of CF before and after depositing EG are observed by SEM. For easy comparison, the CF loading with EG content of 0, 0.5, 1, and 1.5 wt% is chosen as representatives and the images are shown in Fig. 3. After absorbing EG, we can see that a new hierarchical structure is formed [31]. However, no bond is created between EG and CF because of the fact that there are little functionalized groups on surfaces of CF and EG. In addition, we

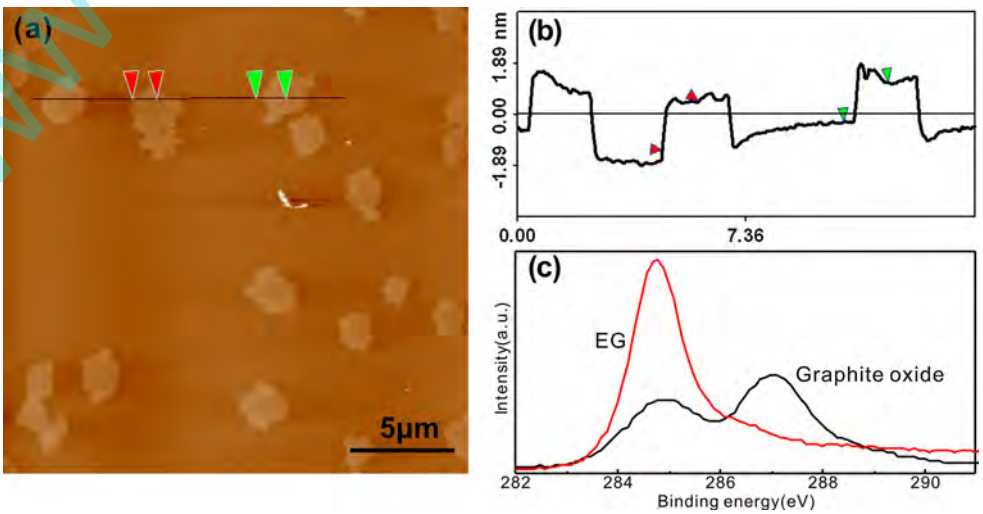

Fig. 2 **a** AFM topographic image, **b** height profiles of EG, and **c** comparison of FT-IR spectra of graphite oxide and EG

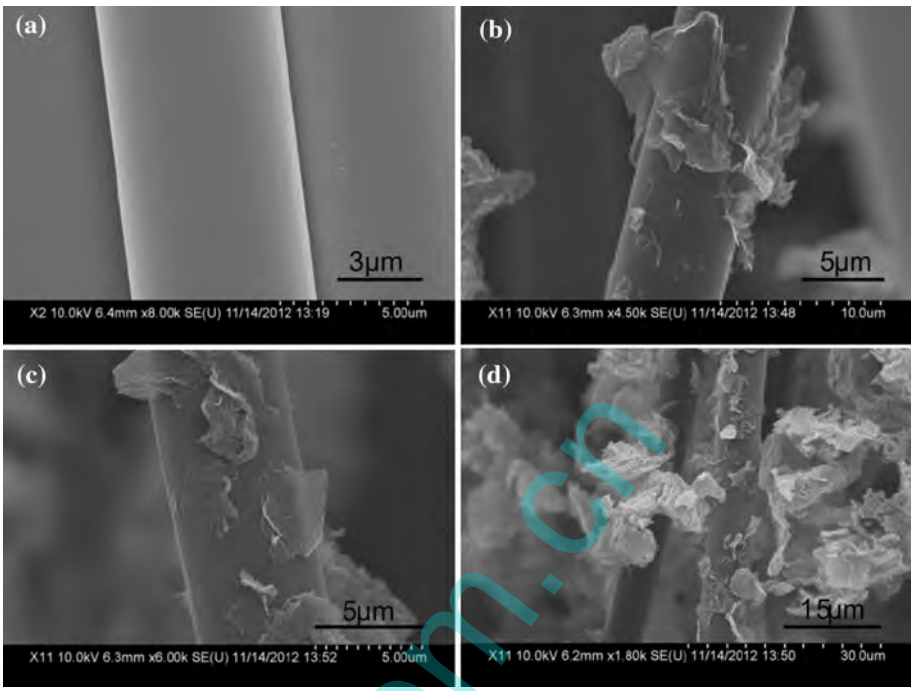

Fig. 3 SEM images of **a** virgin CF and CF deposited by EG with the content of **b** 0.5 wt%, **c** 1 wt%, and **d** 1.5 wt%

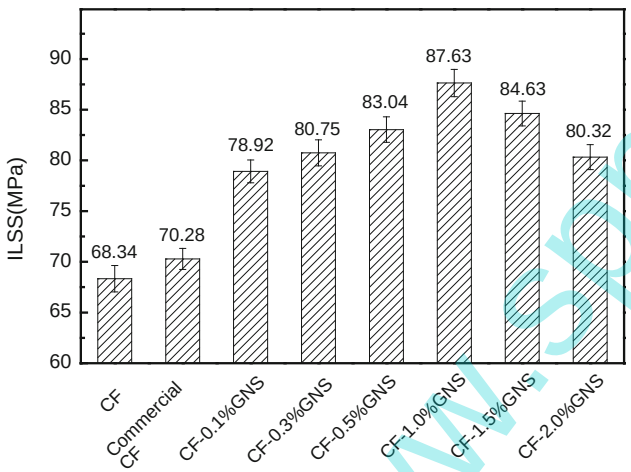

Fig. 4 ILSS of unidirectional composites loading with different contents of EG

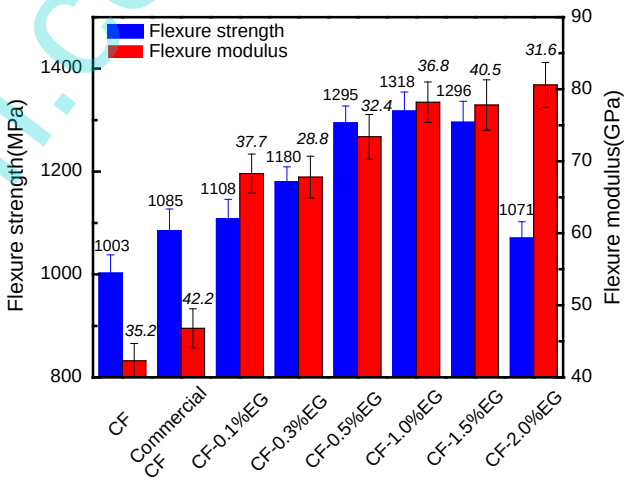

Fig. 5 Flexural performances of unidirectional composites loading with different contents of EG

examine the hierarchical reinforcement and find that most EG are attached along the CF axial direction. Some EG are stably standing on the CF. The size of EG is micro-scale and most of them are irregular. However, there is an obvious agglomeration of EG on the surface of CF with 1.5 wt% EG (Fig. 3d), which may go against the mechanical properties of composites.

Interfacial performance of composites

Interlaminar shear strength is one of the most important parameters for the interfacial performance of composites. The results from the short beam shear tests of the composites with different contents of EG are shown in Fig. 4. All data include statistical deviation. As shown in Fig. 4, all specimens with EG exhibit the improved ILSS in comparison with washed CF and commercial-sized CF-reinforced composites. When the content of EG is lower than 0.1 wt%, reinforcement suffers from low content of EG and results in limited improvement in ILSS. With the increase of EG content, there is a steady improvement of ILSS. Especially, the ILSS of composite with 1 wt% EG is 28.3 % higher than that of baseline sample. This

improvement should be attributed to the increase of the interface layer modulus by adding more EG. However, when the EG loading exceeds 1 wt%, the ILSS is decreased slightly by increasing the EG content. This should be attributed to the fact that a significant amount of EG will agglomerate in interfacial regions (as shown in Fig. 3d) and become stress concentration sites, which decreases the energy dissipating and results in deterioration of interfacial strength [25]. The agglomeration induced decrease of interfacial property is further supported by the decrease of ILSS of hierarchical composites with 2.0 wt% EG.

For further inspecting the enhancing effect of EG on interfacial performance, we investigate flexural properties of composites and the values of flexural strength and flexural modulus are shown in Fig. 5. It is clearly verified that the flexural strength of EG modified composites is greater than that of the composites reinforced by commercial and washed CF. Formation of stronger interface after introducing EG leads to better load transfer from matrix to fibers and results in greater flexural strength. However, excessive EG would aggregate in interfacial phase and new stress concentration sites are formed to decrease the flexural strength. For the flexural modulus of composites toughened by EG, there are some obvious improvements in comparison with that of the pristine composites, showing a trend that is similar to ILSS and flexural strength. Nevertheless, the flexural modulus continues to grow, when EG content exceeds 1 wt%, which

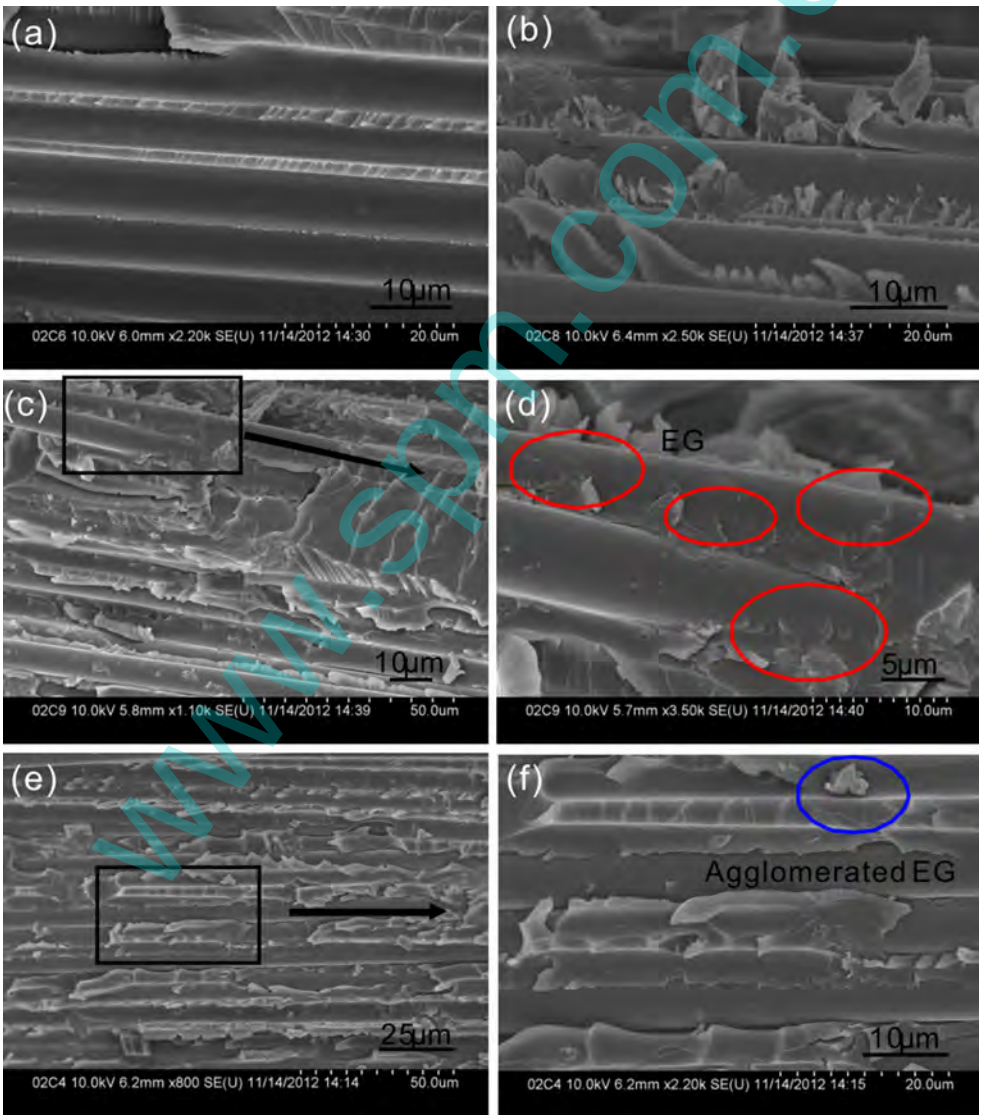

Fig. 6 Fracture surface of **a** pristine composites, **b** hierarchical composites with 0.3 wt% EG, **c** composites with 1 wt% EG and the corresponded parts at higher magnifications in **d**, and **e** composites with 1.5 wt% EG and the corresponded parts at higher magnifications in **f**. *Red circles* in **d** indicate the dispersed EG and *blue circle* in **f** indicated the agglomerated EG (Color figure online)

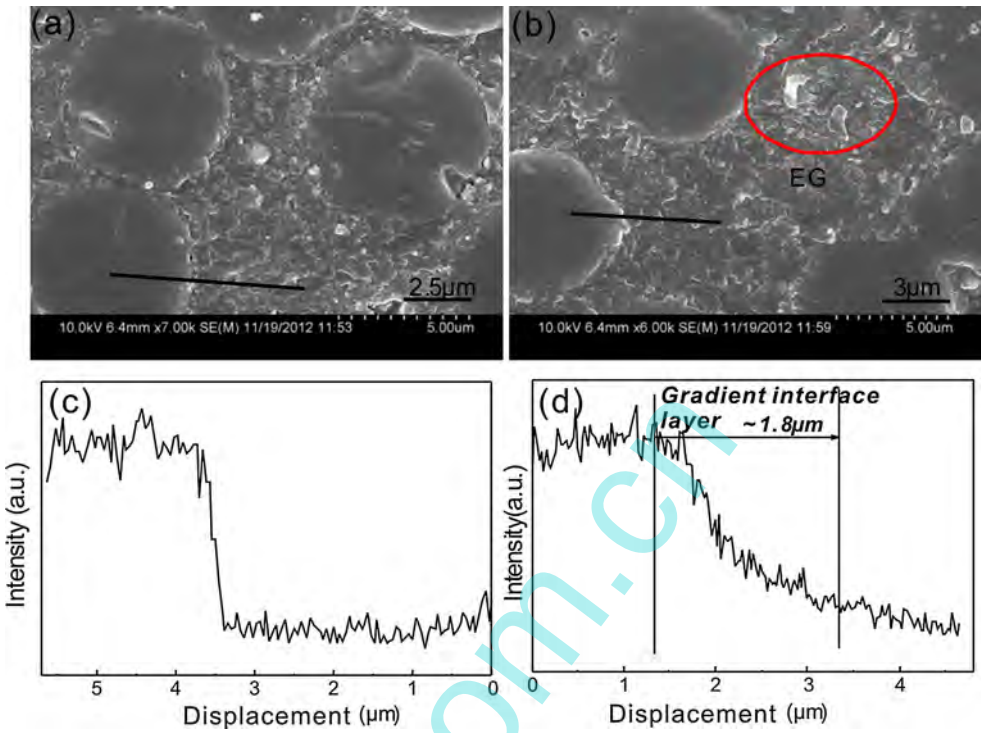

Fig. 7 SEM images of polished fracture surfaces of **a** pristine composites and **b** composites with 1 wt% EG and the corresponding distribution of carbon elements in the interfacial phase of **c** pristine and **d** hierarchical composites

may be attributed to the improvement of matrix modulus after adding excessive EG.

Micrographs of fracture surface

We examine the fracture surfaces of unidirectional composites after flexural tests by SEM to better understand the interface behavior of pristine and modified composites. Figure 6a shows that the fiber surfaces have little matrix adhering to them. The epoxy matrix exhibits a relatively smooth fracture surface, indicating a weak fiber/matrix interface. After adding EG, fracture surface of matrix becomes rough, which is considered to be brought by the decrease of stress concentration (as shown in Fig. 6b). With the increase of EG content (Fig. 6c, d), the matrix fracture surface is found to be much rougher due to the well-dispersed EG indicated by red circles in Fig. 6d, which would lead to increased load transfer efficiency and then a gradual increase in ILSS. Nevertheless, the roughness of composite is seen to be decreased when EG loading is 1.5 wt% (Fig. 6e, f). This should be attributed to the agglomeration of excessive EG (as shown by blue circle in Fig. 6f), which brings about local stress concentration, decreases energy dissipation capability and results in less effective enhancement of the interfacial performance eventually.

Structure of interfacial phase

For the reinforcing mechanisms, little oxygen-containing groups are known on EG, which can rarely form any chemical bonding between EG and fibers or matrix. Moreover, the hydrophobic EG would decrease the fiber surface energy and lead to poor wettability with viscous matrix. Hence, a gradient interface layer which is similar to biological systems and rarely exhibits vastly different mechanical properties [32, 33] is considered to be constructed at the interfacial phase of CF and epoxy resin. It may eventually be beneficial to decrease stress concentration and raise the mechanical properties of composites [34–36].

To verify the introduction of gradient interface layer, the interfacial phase structures of the pristine and the multiscale composites loading with 1 wt% EG are detected in detail. Linear scanning system of SEM is used to evaluate the element distribution in interface region and the results are shown in Fig. 7. As illustrated in Fig. 7c, a sudden drop in the amount of carbon element can be observed from fiber to matrix. However, this drop tendency becomes much slower after addition of EG (Fig. 7d), which demonstrates the formation of nanocomposite interface layer reinforced by EG in the CF/epoxy interfacial phase. In addition, carbon element content dwindles steadily from fibers to matrix, which indicates the gradient distribution of EG in the nanocomposites and supported the construction of gradient interface layers with a thickness of ~1.8 μm (Fig. 7d).

For further investigation of the interfacial phase structures of composites, the force modulation mode of AFM is adopted to study the stiffness of various phases in unidirectional CF/epoxy composites, which allowed a

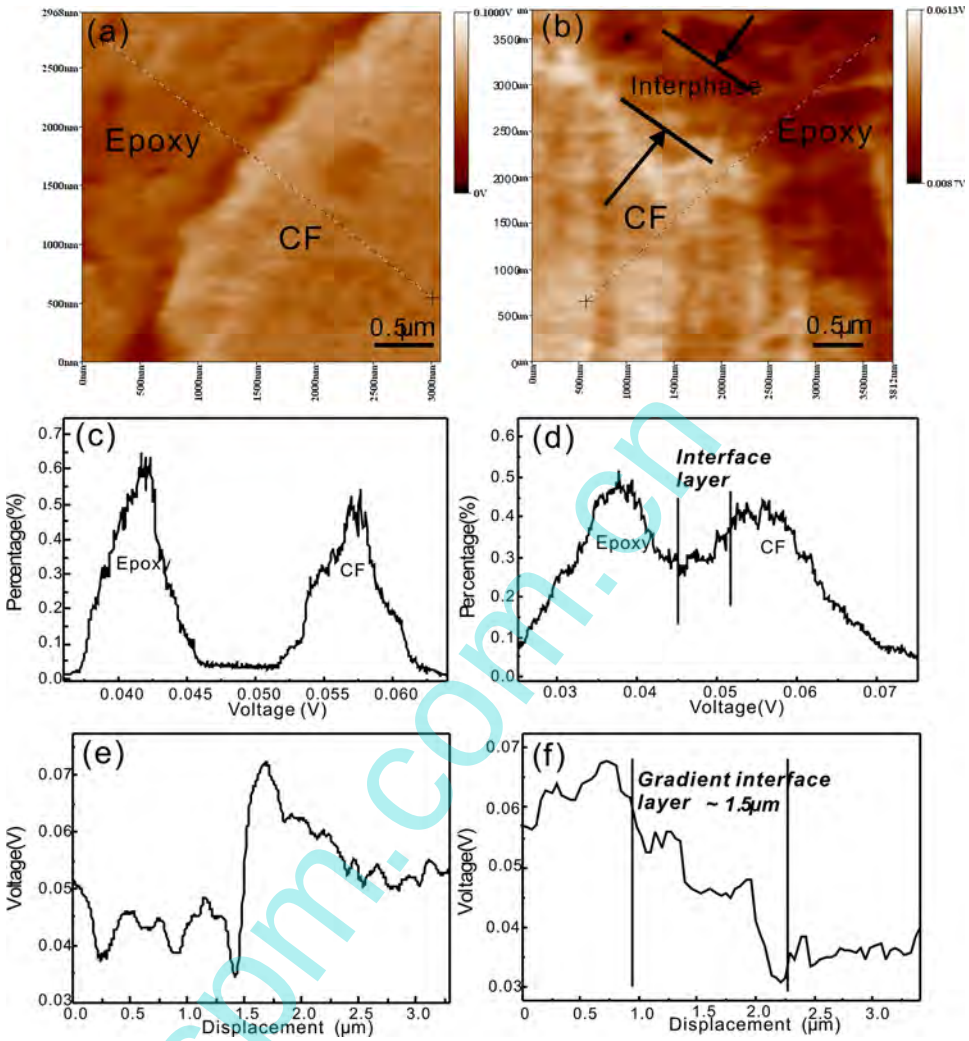

Fig. 8 **a** Relative stiffness images, **c** probability histograms of relative stiffness and **e** stiffness change tendency of untreated composite surface. **b**, **d** and **f** were the corresponding characterizations for hierarchical composite surface

qualitative statement about the local modulus of sample surface using an oscillating cantilever tip that indents into the sample surface. The corresponding cantilever amplitude will change under scanning in accordance with the local modulus of sample. The indentation will be larger on compliant areas, while smaller on stiff areas of the sample. Thus, different responses of the cantilever from areas with different moduli could be observed [36–38].

The force modulation AFM results are shown in Fig. 8. Figure 8a shows apparent contrast between fiber and matrix region. After incorporation of EG, the boundary of CF and epoxy becomes blurrier and an obvious interphase is found as shown in Fig. 8b. Figure 8c, d shows the probability histograms of the relative stiffness. From Fig. 8c, it can be seen that the stiffness distribution curve is clearly divided into two peaks and no obvious transition can be found, indicating two diverse stiffness phases around the interface, and the stiffness of CF(0.052–0.062 V) is much higher than that of epoxy(0.037–0.045 V). However, after adding EG, a new phase with the stiffness values located between 0.045 and 0.052 V, which are all lower than CF, but higher than matrix is emerged (Fig. 8d), which means that an interfacial phase is constructed between CF and matrix. The structures of interfacial phases for pristine and modified composites are further studied in Fig. 8e, f. There is a sharp drop of the stiffness from fiber to epoxy for the pristine composites. Nevertheless, this drop becomes more anetic after adding EG, which implies the introduction of gradient interface layer and is in good agreement with the linear SEM results. The interphase thickness value is ~1.5 μm in Fig. 8f, which is little smaller than that in Fig. 7d due to disparity of samples and experimental errors. This gradient interfacial phase in the composites is similar to biological system, which rarely exhibits discrete boundaries between two materials with vastly different mechanical properties [32, 36]. Therefore, the stress concentration between fiber and matrix would be decreased significantly so that the mechanical properties of composites such as ILSS and flexural strength would show impressive improvements after introducing this gradient interface layer.

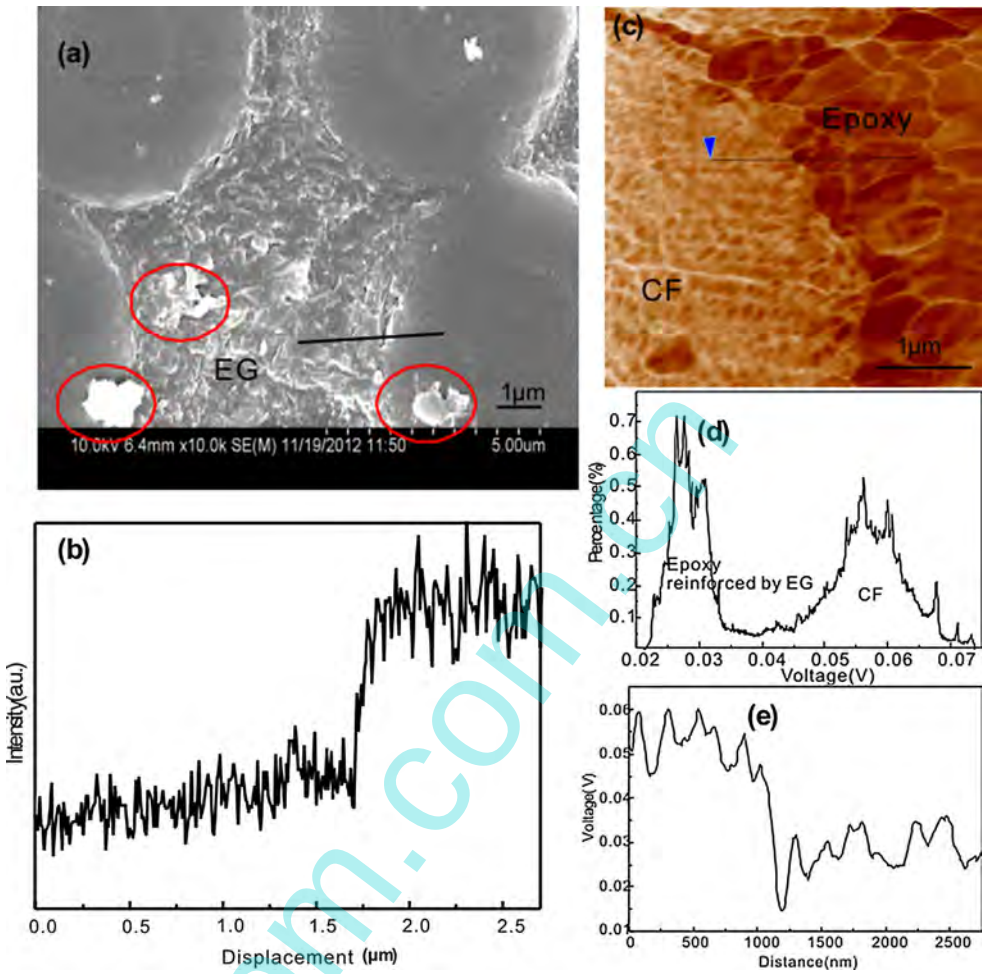

Fig. 9 **a** SEM images of polished fracture surfaces and **b** the distribution of carbon elements in the interfacial phase of sonicated composites. **c** Relative stiffness images, **d** probability histograms of relative stiffness, and **e** stiffness change tendency in sonicated composite surface

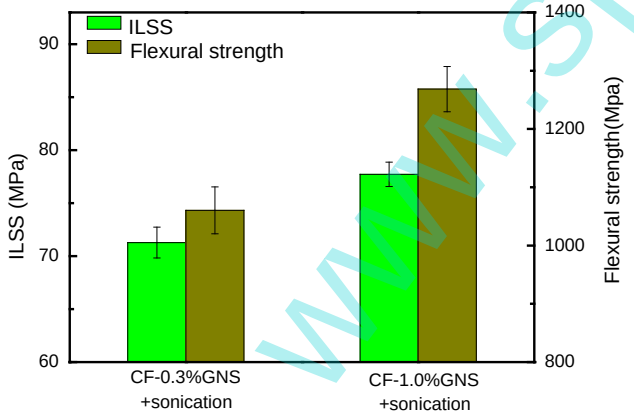

Fig. 10 ILSS and flexural strength of pristine, hierarchical, and sonicated composites

To assure the reinforcing mechanisms of improved load transfer efficiency by introducing gradient interface layers rather than stiffening of locally matrix properties by adding EG, we prepare multi-scale composites with EG dispersed homogeneously in matrix by sonication. The interface structures are also detected using SEM and force modulation AFM in Fig. 9. Compared with Fig. 7d, Fig. 9b shows that an apparent contrast of carbon element distribution is re-appeared after sonication. In addition, modulus is dropped sharply from fiber to matrix (Fig. 9e) and gradient interphase region cannot be found from Fig. 9c, d. All of these prove that the EG are dispersed uniformly into the matrix so that the gradient structures are vanished after sonication. ILSS and flexural properties of the sonicated composites with 0.3 and 1 wt% EG are measured and calculated and the results are shown in Fig. 10. It can be clearly seen that the disappearance of gradient interphase decrease the ILSS and flexural properties of hierarchical composites, which confirms the positive effect of gradient interphase on the interfacial properties from a different angle. The exact structure differences between the pristine, hierarchical, and sonicated composites are illustrated in Fig. 11.

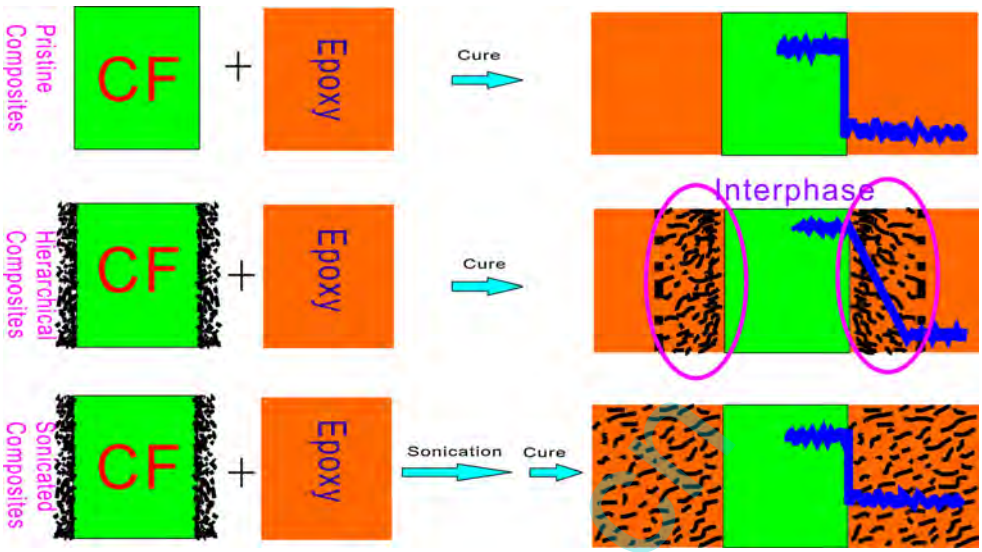

Fig. 11 Schema for the differences between pristine, hierarchical, and sonicated composites

Conclusions

To improve the interfacial properties of CF/epoxy composites, EG were delivered to the surface of CF by a liquid phase deposition method. A gradient interface layer reinforced by EG is established successfully in interfacial phase during the forming process of composites. Due to the formation of this gradient interface layer, 28.3 % enhancement of unidirectional CF/epoxy composites in ILSS is observed with EG loading of 1 wt%. The flexural properties of the composites are also enhanced owing to the improved interfacial performance. Based on the linear scanning system of SEM and the force modulation mode of AFM, the exact structure of this gradient interfacial phase is detected. After adding EG, the modulus drop from CF to matrix is found to be slowed significantly. This plays an important role for improving stress transformation from CF to epoxy and then enhancing the interfacial performance. However, when EG loading exceeds 1.5 wt%, ILSS and flexural strength are shown to be decreased, which may be attributed to the reappearance of stress concentration induced by agglomeration of excess EG. To verify the effect of gradient interphase on the interfacial properties of composites from a different angle, the gradient interphase is removed by sonicating the uncured composites with EG. Gradient interphase structures are disappeared and interfacial performance of composites is found to be weakened, which further confirmed the capacity of decreasing stress concentration by gradient interfacial layers.

In our present work, 28.3 % increase of the ILSS is smaller than that reported in the literatures [13, 21, 36, 39]. However, the preparing procedures of our hierarchical CF/EG reinforced multi-scale composites, whose interfacial performance is improved due to the introduction of gradient interfacial phase, rather than the reported mechanisms of creating chemical bonding or mechanical interlocking or increasing fiber surface area, can be realized for industrial production. In addition, further regulating the structures of gradient interfacial phases, such as functionalizing EG, using other nanomaterials to replace EG or altering the width of gradient interface, is expected to be a promising strategy to improve the interfacial performance significantly.

Acknowledgements The authors acknowledge the financial support from National Natural Science Foundation of China (U1362108, 11175130), and Natural Science Foundation of Tianjin, China (10JCYBJC02300).

References

1. Zhang XQ, Fan XY, Yan C et al (2012) Interfacial microstructure and properties of carbon fiber composites modified with graphene oxide. Acs Appl Mater Interf 4:1543–1552. doi:10.1021/am201757v
2. Yavari F, Rafiee MA, Rafiee J, Yu ZZ, Koratkar N (2010) Dramatic increase in fatigue life in hierarchical graphene composites. Acs Appl Mater Interf 2:2738–2743. doi:10.1021/am100728r
3. Kim M, Park Y-B, Okoli OI, Zhang C (2009) Processing, characterization, and modeling of carbon nanotube-reinforced multi-scale composites. Compos Sci Technol 69:335–342. doi:10.1016/j.compscitech.2008.10.019
4. Peng Q, He X, Li Y et al (2012) Chemically and uniformly grafting carbon nanotubes onto carbon fibers by poly(amido-amine) for enhancing interfacial strength in carbon fiber composites. J Mater Chem 22:5928–5931. doi:10.1039/c2jm16723a
5. Chou T-W, Gao L, Thostenson ET, Zhang Z, Byun J-H (2010) An assessment of the science and technology of carbon nanotube-based fibers and composites. Compos Sci Technol 70:1–19. doi:10.1016/j.compscitech.2009.10.004
6. Yokozeki T, Iwahori Y, Ishibashi M et al (2009) Fracture toughness improvement of CFRP laminates by dispersion of cup-

stacked carbon nanotubes. Compos Sci Technol 69:2268–2273. doi:10.1016/j.compscitech.2008.12.017
7. Yang XL, Wang ZC, Xu MZ, Zhao R, Liu XB (2013) Dramatic mechanical and thermal increments of thermoplastic composites by multi-scale synergetic reinforcement: carbon fiber and graphene nanoplatelet. Mater Des 44:74–80. doi:10.1016/j.matdes.2012.07.051
8. He X, Zhang F, Wang R, Liu W (2007) Preparation of a carbon nanotube/carbon fiber multi-scale reinforcement by grafting multi-walled carbon nanotubes onto the fibers. Carbon 45:2559–2563. doi:10.1016/j.carbon.2007.08.018
9. Green KJ, Dean DR, Vaidya UK, Nyairo E (2009) Multiscale fiber reinforced composites based on a carbon nanofiber/epoxy nanophased polymer matrix: synthesis, mechanical, and thermomechanical behavior. Compos Part A 40:1470–1475. doi:10.1016/j.compositesa.2009.05.010
10. Arai M, Noro Y, Sugimoto K-I, Endo M (2008) Mode I and mode II interlaminar fracture toughness of CFRP laminates toughened by carbon nanofiber interlayer. Compos Sci Technol 68:516–525. doi:10.1016/j.compscitech.2007.06.007
11. Sager RJ, Klein PJ, Lagoudas DC et al (2009) Effect of carbon nanotubes on the interfacial shear strength of T650 carbon fiber in an epoxy matrix. Compos Sci Technol 69:898–904. doi:10.1016/j.compscitech.2008.12.021
12. Thostenson ET, Li WZ, Wang DZ, Ren ZF, Chou TW (2002) Carbon nanotube/carbon fiber hybrid multiscale composites. J Appl Phys 91:6034–6037. doi:10.1063/1.1466880
13. Bekyarova E, Thostenson ET, Yu A et al (2007) Multiscale carbon nanotube-carbon fiber reinforcement for advanced epoxy composites. Langmuir 23:3970–3974. doi:10.1021/la062743p
14. Wicks SS, de Villoria RG, Wardle BL (2010) Interlaminar and intralaminar reinforcement of composite laminates with aligned carbon nanotubes. Compos Sci Technol 70:20–28. doi:10.1016/j.compscitech.2009.09.001
15. Garcia EJ, Wardle BL, Hart AJ, Yamamoto N (2008) Fabrication and multifunctional properties of a hybrid laminate with aligned carbon nanotubes grown in situ. Compos Sci Technol 68:2034–2041. doi:10.1016/j.compscitech.2008.02.028
16. Zhang F-H, Wang R-G, He X-D, Wang C, Ren L-N (2009) Interfacial shearing strength and reinforcing mechanisms of an epoxy composite reinforced using a carbon nanotube/carbon fiber hybrid. J Mater Sci 44:3574–3577. doi:10.1007/s10853-009-3484-x
17. Tehrani M, Boroujeni AY, Hartman TB, Haugh TP, Case SW, Al-Haik MS (2013) Mechanical characterization and impact damage assessment of a woven carbon fiber reinforced carbon nanotube-epoxy composite. Compos Sci Technol 75:42–48. doi:10.1016/j.compscitech.2012.12.005
18. Sanchez M, Campo M, Jimenez-Suarez A, Urena A (2013) Effect of the carbon nanotube functionalization on flexural properties of multiscale carbon fiber/epoxy composites manufactured by VARIM. Compos Part B 45:1613–1619. doi:10.1016/j.compositesb.2012.09.063
19. Li M, Gu Y, Liu Y, Li Y, Zhang Z (2013) Interfacial improvement of carbon fiber/epoxy composites using a simple process for depositing commercially functionalized carbon nanotubes on the fibers. Carbon 52:109–121. doi:10.1016/j.carbon.2012.09.011
20. Zhu Y, Bakis CE, Adair JH (2012) Effects of carbon nanofiller functionalization and distribution on interlaminar fracture toughness of multi-scale reinforced polymer composites. Carbon 50:1316–1331. doi:10.1016/j.carbon.2011.11.001
21. Zhao F, Huang Y (2011) Preparation and properties of polyhedral oligomeric silsesquioxane and carbon nanotube grafted carbon fiber hierarchical reinforcing structure. J Mater Chem 21:2867–2870. doi:10.1039/c0jm03919e
22. Rodriguez AJ, Guzman ME, Lim C-S, Minaie B (2011) Mechanical properties of carbon nanofiber/fiber-reinforced hierarchical polymer composites manufactured with multiscale-reinforcement fabrics. Carbon 49:937–948. doi:10.1016/j.carbon.2010.10.057
23. Liang J, Wang Y, Huang Y et al (2009) Electromagnetic interference shielding of graphene/epoxy composites. Carbon 47:922–925. doi:10.1016/j.carbon.2008.12.038
24. Qiu JJ, Wang SR (2011) Enhancing polymer performance through graphene sheets. J Appl Polym Sci 119:3670–3674. doi:10.1002/app.33068
25. Rafiq R, Cai D, Jin J, Song M (2010) Increasing the toughness of nylon 12 by the incorporation of functionalized graphene. Carbon 48:4309–4314. doi:10.1016/j.carbon.2010.07.043
26. Stankovich S, Dikin DA, Dommett GHB et al (2006) Graphene-based composite materials. Nature 442:282–286. doi:10.1038/nature04969
27. Bortz DR, Heras EG, Martin-Gullon I (2012) Impressive fatigue life and fracture toughness improvements in graphene oxide/epoxy composites. Macromolecules 45:238–245. doi:10.1021/ma201563k
28. Rafiee MA, Rafiee J, Srivastava I et al (2010) Fracture and fatigue in graphene nanocomposites. Small 6:179–183. doi:10.1002/smll.200901480
29. Marcano DC, Kosynkin DV, Berlin JM et al (2010) Improved synthesis of graphene oxide. ACS Nano 4:4806–4814. doi:10.1021/Nn1006368
30. McAllister MJ, Li J-L, Adamson DH et al (2007) Single sheet functionalized graphene by oxidation and thermal expansion of graphite. Chem Mater 19:4396–4404. doi:10.1021/cm0630800
31. Akhavan O, Ghaderi E, Rahighi R (2012) Toward single-DNA electrochemical biosensing by graphene nanowalls. ACS Nano 6:2904–2916. doi:10.1021/nn300261t
32. Lin Y, Ehlert G, Sodano HA (2009) Increased interface strength in carbon fiber composites through a ZnO nanowire interphase. Adv Funct Mater 19:2654–2660. doi:10.1002/adfm.200900011
33. Ishida H, Chaisuwan T (2003) Mechanical property improvement of carbon fiber reinforced polybenzoxazine by rubber interlayer. Polym Compos 24:597–607. doi:10.1002/pc.10056
34. Cech V (2007) Plasma-polymerized organosilicones as engineered interlayers in glass fiber/polyester composites. Compos Interf 14:321–334. doi:10.1163/156855407780452850
35. Yao Y, Chen SH, Chen PJ (2013) The effect of a graded interphase on the mechanism of stress transfer in a fiber-reinforced composite. Mech Mater 58:35–54. doi:10.1016/j.mechmat.2012.11.008
36. Zhao F, Huang Y, Liu L, Bai Y, Xu L (2011) Formation of a carbon fiber/polyhedral oligomeric silsesquioxane/carbon nanotube hybrid reinforcement and its effect on the interfacial properties of carbon fiber/epoxy composites. Carbon 49:2624–2632. doi:10.1016/j.carbon.2011.02.026
37. Eitan A, Fisher FT, Andrews R, Brinson LC, Schadler LS (2006) Reinforcement mechanisms in MWCNT-filled polycarbonate. Compos Sci Technol 66:1162–1173. doi:10.1016/j.compscitech.2005.10.004
38. Munz M, Sturm H, Schulz E, Hinrichsen G (1998) The scanning force microscope as a tool for the detection of local mechanical properties within the interphase of fibre reinforced polymers. Compos Part A 29:1251–1259. doi:10.1016/s1359-835x(98)00077-3
39. Fan Z, Santare MH, Advani SG (2008) Interlaminar shear strength of glass fiber reinforced epoxy composites enhanced with multi-walled carbon nanotubes. Compos Part A 39:540–554. doi:10.1016/j.compositesa.2007.11.013